Acyl transfer from carboxylate, carbonate, and thiocarbonate esters to enzymatic and nonenzymatic thiolates

Christian Gravel, Danielle Lapierre, Judith Labelle, and Jeffrey W. Keillor

Abstract: Transglutaminases (EC 2.3.2.13) (TGases) catalyze calcium-dependent acyl transfer reactions between peptide-bound glutamine residues as acyl donors and peptide-bound lysine residues as acyl acceptors, resulting in the formation of intermolecular ε-(γ-glutamyl)lysine crosslinks. The mechanistic details of its "ping-pong" transamidation reaction remain unknown. In particular, few studies have been published probing the nucleophilicity of TGase using acyl-donor substrates of varied electrophilicity. Herein we report the synthesis of activated esters of carbonates, carbamates, and thiocarbonates and their reactions with simple thiols, as a nonenzymatic point of reference, and with the catalytic cysteine residue of guinea pig liver TGase. Our kinetic results show that the simple substitution of a side chain methylene unit by oxygen or sulphur had a surprising effect on both substrate affinity and acylation reactivity. Furthermore, they provide unexpected insight into the importance of a side chain heteroatom for conferring affinity for tissue TGase as well as revealing an interesting class of irreversible inhibitors.

Key words: enzyme kinetics, enzyme inhibition, transglutaminase, acyl-transfer reactions, carbamate, thiocarbonate, carbonate.

Résumé : Les transglutaminases (EC 2.3.2.13) (TGases) catalysent, avec dépendance au calcium, le transfert d'un groupement acyle entre les résidus glutamine d'une première protéine et les résidus lysine d'une seconde protéine. Ceci résulte en la formation de réticulation intermoléculaire du type ε-(γ-glutamyl)lysine. Les détails mécanistiques de sa réaction de transamidation de type « ping-pong » restent inconnus. En particulier, peu d'études explorant la nucléophilie de la TGase à l'aide de substrats donneurs d'électrophilie variable ont été publiées. Dans cet article, nous rapportons la synthèse des esters activés des carbonates, carbamates et thiocarbonates ainsi que leurs réactions avec des thiols simples, comme point de référence non-enzymatique, et avec la cystéine catalytique de la TGase de foie de cobaye. Nos résultats cinétiques démontrent que la substitution simple d'un groupement méthylène par un oxygène ou par un soufre a un effet surprenant sur l'affinité de substrat ainsi que sur la réactivité d'acylation. De plus, ils permettent un aperçu inattendu de l'importance de la présence d'un hétéroatome dans la chaîne latérale pour conférer l'affinité pour la TGase tissulaire et révèlent une classe d'inhibiteurs irréversibles intéressants.

Mots-clés : cinétique enzymatique, inhibition d'enzyme, transglutaminase, transfert de groupement acyle, carbamate, thiocarbonate, carbonate.

Introduction

Transglutaminases (EC 2.3.2.13) (TGases) belong to a class of enzymes known as aminoacyltransferases that catalyze calcium-dependent acyl transfer reactions between peptide-bound glutamine residues as acyl donors and peptide-bound lysine residues as acyl acceptors, resulting in the formation of intermolecular ε-(γ-glutamyl)lysine crosslinks (1). TGases form a family of related enzymes found in plasma, tissues, and extracellular media in all vertebrates. One of the best known TGases is the well-characterized human plasma coagulation enzyme Factor XIIIa, activated by thrombin from its tetrameric zymogen during the coagulation process (2, 3). Other types of TGase known to date include the keratinocyte TGase (type I) (4), two epidermal TGases (types III and V), a TGase localized in the prostate (type IV) (5, 6), and the ubiquitous tissue TGase (type II), the focus of our research interest. Guinea pig liver tissue TGase (gTGase) was chosen as a model of the human enzyme for this work because it is 88% homologous (7) to the human tissue TGase (hTGase) and is readily purified in its recombinant His-tagged form (8). gTGase is a monomeric protein comprising 690 amino acids with a calculated molecular weight of 78.7 kDa. It is not glycosylated (1) although it possesses six potential *N*-glycosylation sites and contains 17 cysteine residues, none of which are comprised in disulfide bonds (9). One of these acts as the catalytic nucleophile, in a Cys-His-Asp triad reminiscent of that of the cysteine proteases. Comparison of the amino acid sequence of gTGase with those of the only TGases for which X-ray structures are

Received 18 December 2006. Accepted 5 February 2007. Published on the NRC Research Press Web site at http://canjchem.nrc.ca on 15 March 2007.

C. Gravel,[1] D. Lapierre,[1] J. Lavelle, and J. W. Keillor.[2] Département de chimie, Université de Montréal, CP 6128, Succursale centre-ville, Montréal, QC H3C 3J7, Canada.

[1]These authors contributed equally to this work.
[2]Corresponding author (e-mail: jw.keillor@umontreal.ca).

 doi:10.1139/V07-011

available — Factor XIIIa (10), human epidermal Tgase (eTGase) (11), human tissue TGase (hTGase) (12), and a fish tissue TGase (fTGase) (13) — indicates that the catalytic triad of gTGase would be composed of Cys-276, His-334, and Asp-358. The catalytic acyl-transfer reaction is known to proceed through a modified "ping-pong" mechanism (14) that is yet to be completely understood despite the involvement of TGase in critical processes such as the stabilization of extracellular matrices, formation of cross-linked cell envelopes, cell-matrix assembly, wound healing, and cellular adhesive processes (1). TGase has been implicated in important physiological disorders, such as amyloid protein aggregation leading to Alzheimer's disease (15), thrombosis, arteriosclerosis (16), autoimmune gluten intolerance (Celiac disease) (17, 18), cataract development (19), and Hb-Koln disease (2). TGase has also been implicated in neurodegenerative diseases related to an increase in transamidated (20) polyglutamine-containing peptide, leading to aggregation in neural tissues such as Huntington's disease (21). In the ping-pong mechanism, the acyl donor substrate undergoes nucleophilic attack by the active site thiolate, followed by the release of an equivalent of ammonia. The thiolester acyl enzyme intermediate thus obtained then undergoes a second nucleophilic attack by the acyl acceptor substrate, typically a primary amine, leading to the formation of a new isopeptidic compound and the regeneration of the free enzyme. These steps are facilitated by the presence of a general acid–base catalyst, His-334 (22). Water can also compete weakly as an acyl acceptor during the deacylation step, resulting in the net hydrolysis of the initial acyl-donor amide.

While a significant amount of data is available regarding the specificity and reactivity of various glutamine substrates (23, 24), far fewer studies have been published probing the nucleophilicity of TGase using acyl-donor substrates of varied electrophilicity. In addressing this paucity of data we carried out kinetic studies with nonenzymatic thiols to provide a point of reference. The thermal decomposition of such esters (25) and their susceptibility to nucleophilic attack by phenolate, secondary acyclic amines, and pyridines have been reported (26, 27, 28), but kinetic studies concerning the acylation of simple thiols by carboxylate-, carbonate-, carbamate-, and thiocarbamate-esters are also relatively few (29, 30). Herein we report on the reaction of the activated esters of carbonates, carbamates, and thiocarbonates with simple thiols and the catalytic cysteine residue of gTGase.

Results and discussion

Design and synthesis of acyl-donor reactants

Compounds **1**, **2**, and **3** (see Fig. 1) were designed to bear the essential structural elements required for recognition by TGase as an acyl-donor substrate, i.e., a hydrophobic, planar moiety on the *N*α of the glutamine residue, a central amino acid having L configuration (31), and at least two methylene units in its side chain (asparagine not being recognized as a substrate) (22, 32, 33). The C-terminal glycine residue is not absolutely required but improves binding by an order of magnitude probably by distancing the terminal negative charge from the carboxylate of the central amino acid (33). Compounds **4**, **5**, and **6** (Fig. 1) were chosen as simplified

Fig. 1. Acyl-donor reactants studied herein.

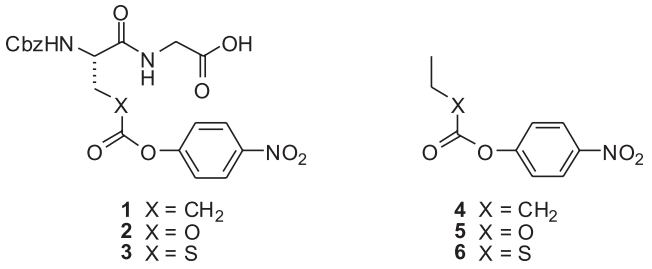

functional models because of their commercial availability or synthetic accessibility as well as their resemblance to the reactive side chains of **1**, **2**, and **3**. Although it may have been interesting to study the acylation TGase from *p*-nitrophenyl carbamates (e.g., X = NH in Fig. 1), we confirmed that these molecules undergo a rapid elimination reaction in water releasing *p*-nitrophenolate and generating the corresponding isocyanate (34, 35, 36, 37), making their kinetic study impossible.

Compound **1** was synthesized as described previously (22). Compounds **2** and **3** were synthesized according to the pathways shown in Schemes 1 and 2, respectively. These synthetic routes are both straightforward, consisting of an initial protection of the amino groups of either serine (for compound **2**) or cystine (for compound **3**) with benzyl chloroformate (Cbz–Cl), followed by peptide coupling using TBTU as a coupling agent and subsequent introduction of the *p*-nitrophenoxycarbonyl moiety. In the case of compound **3**, a reduction step was required prior to side chain functionalization. Finally, deprotection of the *tert*-butyl ester provided the desired compounds **2** and **3** in modest unoptimized yields (34% and 40% overall isolated yields, respectively) but in quantities sufficient for subsequent kinetic studies.

Compound **4** is commercially available (Sigma-Aldrich) and compounds **5** and **6** were obtained by following known protocols (38, 39) in which *p*-nitrophenolate reacts with ethyl chloroformate and ethyl thiochloroformate with yields of 77% and 94%, respectively (Scheme 3).

Nonenzymatic kinetics

The reactions of ester **4**, carbonate **5**, and thiocarbonate **6** with either ethanethiol or cysteamine were followed spectrophotometrically by monitoring the increase in absorbance at 410 nm due to released *p*-nitrophenol. Under pseudo first-order conditions with thiol concentrations over 10-fold higher than those of compounds **4**–**6**, reaction kinetics were found to be clean first-order over at least five half-lives, allowing the determination of pseudo first-order rate constants (k_{obs}) by fitting the absorbance data to a simple mono-exponential equation (see Experimental section). The variation of k_{obs} as a function of thiol concentration provided the second order rate constants (k_2) for each of the thiolysis reactions studied. Figure 2 shows a representative example.

Second-order rate constants were thus obtained using either cysteamine or ethanethiol as nucleophiles at both pH 7 and 8. The results, shown in Table 1, demonstrate the greater reactivity of both thiols at higher pH, consistent with the thiolate being the active nucleophile. Also shown in bold in Table 1 are second-order rate constants normalized for the

Scheme 1. Synthesis of *N*-benzyloxycarbonyl-*O*-(*p*-nitrophenyloxycarbonyl)-L-serinylglycine (**2**). (**a**) CbzCl, aq. $NaHCO_3$, RT, overnight, 58%; (**b**) GlyOtBu, TBTU, DIEA, ACN, RT, overnight, 94%; (**c**) pNPCOCl, Et_3N, ACN, 0 °C, 3 h, 63%; (**d**) TFA, CH_2Cl_2, 0 °C, 1 h, quantitative.

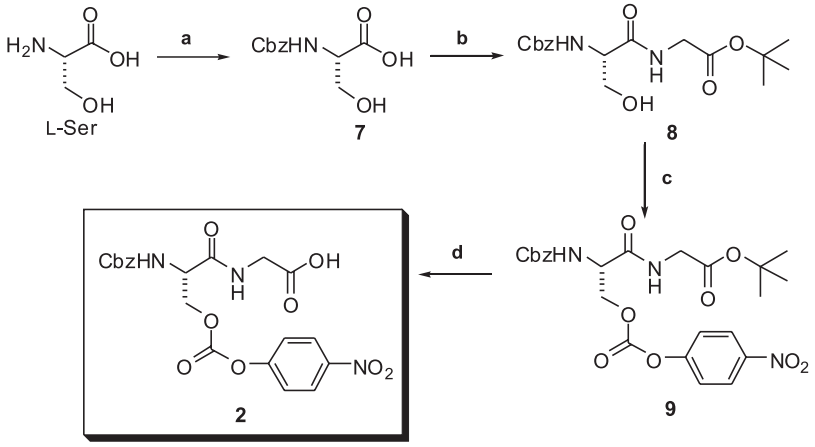

Scheme 2. Synthesis of *N*-benzyloxycarbonyl-*S*-(*p*-nitrophenyloxycarbonyl)-L-cysteinylglycine (**3**). (**a**) CbzCl, aq. $NaHCO_3$, RT, overnight, 99%; (**b**) GlyOtBu, TBTU, DIEA, ACN, RT, overnight, 60%; (**c**) $NaBH_4$, ethanol–$CHCl_3$, RT, 30 min, quantitative; (**d**) pNPCOCl, DIEA, $CHCl_3$, 0 °C, 15 min, 68%; (**e**) TFA, $CHCl_3$, 0 °C, 1 h, quantitative.

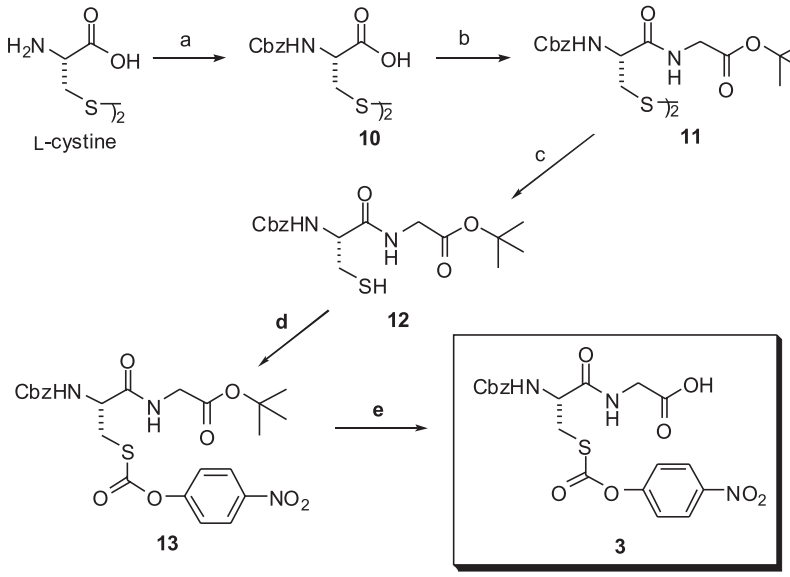

Scheme 3. Synthesis of ethyl *p*-nitrophenyl formate (**5**) and *S*-ethyl *p*-nitrophenyl thioformate (**6**). For compound (**5**), **a**: sodium *p*-nitrophenoxyde, acetonitrile, 0 °C, 30 min, 77%; for compound (**6**), **a**: *p*-nitrophenol, pyridine, CH_2Cl_2, 0 °C, 16 h, 94%.

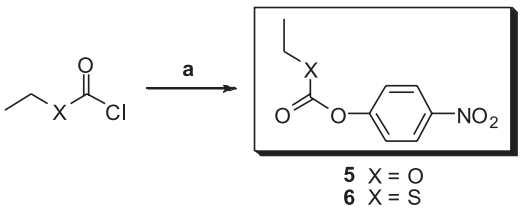

5 X = O
6 X = S

fraction of thiolate present at each pH, based on literature values for the corresponding pK_a values (34, 35). This normalization generates similar values at each pH, within experimental error, for most of the compounds studied.

It is also clear from Table 1 that ester **4** reacts most rapidly with both thiols, followed by thiocarbonate **6** and (or) carbonate **5**. This trend in their relative reactivity most likely reflects their relative electrophilicity and a rate-limiting step involving nucleophilic attack by thiolate. In support of this supposition of relative electrophilicity, the ^{13}C chemical shifts of the side chain carbonyl groups of compounds **4**–**6**, indicative of their relative deshielding or electron density, are noted to be 172, 170, and 153 ppm, respectively, following the same general trend as their reactivity. The decreased electrophilicity of derivatives **5** and **6** compared with **4** suggests that resonance stabilization of the carbonyl group through electron donation from an adjacent heteroatom is more important than electron withdrawal through inductive effects.

It is also instructive to compare the relative reactivity of cysteamine and ethanethiol. It is evident from Table 1 that

Table 1. Second-order rate constants (k_2 (mol/L min)$^{-1}$) for the thiolysis of compounds **4**–**6** at 25 °C.

	Cysteamine pK_a = 8.35 and 10.49 (40)		Ethanethiol pK_a = 10.35 (41)	
Reactant	pH 7, f_{RS^-} = 0.043	pH 8, f_{RS^-} = 0.31	pH 7, f_{RS^-} = 4.5×10^{-4}	pH 8, f_{RS^-} = 4.5×10^{-3}
Ester **4**	4.65±0.07	30.4±0.9	0.057±0.004	0.66±0.06
	109±2	**98±3**	**130±9**	**160±16**
Carbonate **5**	1.89±0.03	11.1±0.4	0.035±0.007	0.19±0.01
	44.2±0.7	**36±2**	**78±16**	**42±2**
Thiocarbonate **6**	2.7±0.1	17.9±0.6	0.010±0.006	0.16±0.02
	63±2	**58±2**	**22±13**	**36±4**

Note: Values in boldface are normalized for the fraction of thiolate present at a given pH (f_{RS^-}). Reported experimental errors derive from linear regression of the first-order data.

Fig. 2. Determination of second order rate constants for the thiolysis of ester **4** (squares), carbonate **5** (triangles) and thiocarbonate **6** (circles) upon reaction with cysteamine (35 °C, pH = 7.0). Inset: typical mono-exponential reaction from which k_{obs} was measured.

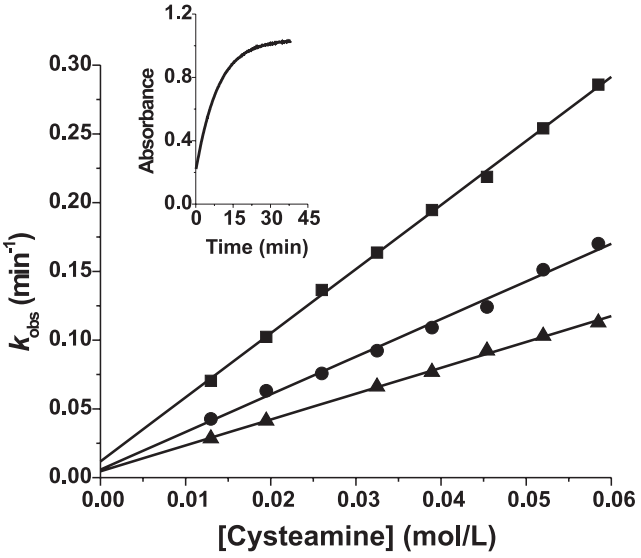

Fig. 3. Acylation of 2.2 μmol/L of gTGase by 198 μM of ester **1** at 25 °C and pH 7.0 (0.1 mol/L MOPS). (See Experimental for background correction.).

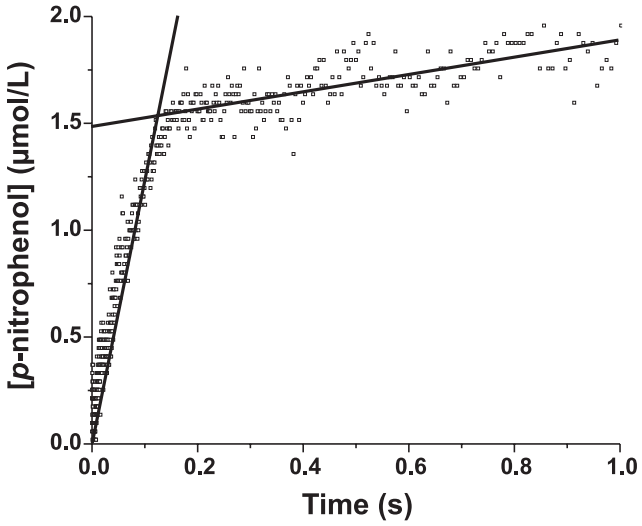

while the presence of a pendant ammonium group serves to decrease the pK_a of the thiol group of cysteamine, it does not further accelerate the reaction of the thiolate form significantly above that of ethanethiol. As has been noted previously, a pendant ammonium group can assist in the thiolysis of amides by acting as an intramolecular general acid protonating an amine leaving group (42). However, it has also been noted that this role is not required for a leaving group such as *p*-nitrophenolate (42, 43), also present in compounds **1**–**6**, whose departure does not require protonation.

Enzymatic kinetics

Compounds **1**–**3** were tested as substrates for recombinant gTGase and found to display similar kinetic behaviour during the first second of reaction. As shown in Fig. 3, rapid release of *p*-nitrophenol corresponding roughly to one equivalent of enzyme (0–0.1 s) was followed by slower turnover (0.1–1.0 s). The pre-steady state "burst" is consistent with the rapid acylation of gTGase by compounds **1**–**3**, leading to the corresponding acyl-enzyme featured in the ping-pong mechanism of Fig. 4. The initial rates of this burst phase were measured as a function of substrate concentration and fitted according to the hyperbolic Michaelis–Menten equation (see Experimental section) as shown in Fig. 5. The kinetic parameters obtained in this fashion are shown in Table 2.

At first glance, it is evident that the kinetic parameters measured for ester **1** and carbonate **2** are similar. Insofar as the K_M values reflect enzyme affinity for the substrate, it is not surprising that this parameter would be similar for the analogous compounds **1** and **2**. Moreover, the slight decrease in the acylation rate constant (k_{acyl}) on passing from the ester to the carbonate is to be expected for the reasons outlined earlier in the discussion of compounds **4** and **5**. Namely, the carbonate ester is presumably less electrophilic than the carboxylate ester as a result of resonance stabilization from the adjacent oxygen atom and therefore less susceptible to nucleophilic attack by the active site thiolate.

However, there is a reversal of this apparent trend on consideration of the kinetic parameters obtained for thiocarbonate **3**. The replacement of the γ-methylene unit of **1** by a sulfur atom in **3** leads to a ~20-fold decrease in the K_M and an increase in the value of k_{acyl}, suggesting a significant increase in affinity. The acylation rate constant itself increases by a factor of ~2.5, resulting in a combined ~50-fold increase in the efficiency of the enzymatic reaction (re-

Fig. 4. Ping-pong mechanism of TGase catalytic cycle.

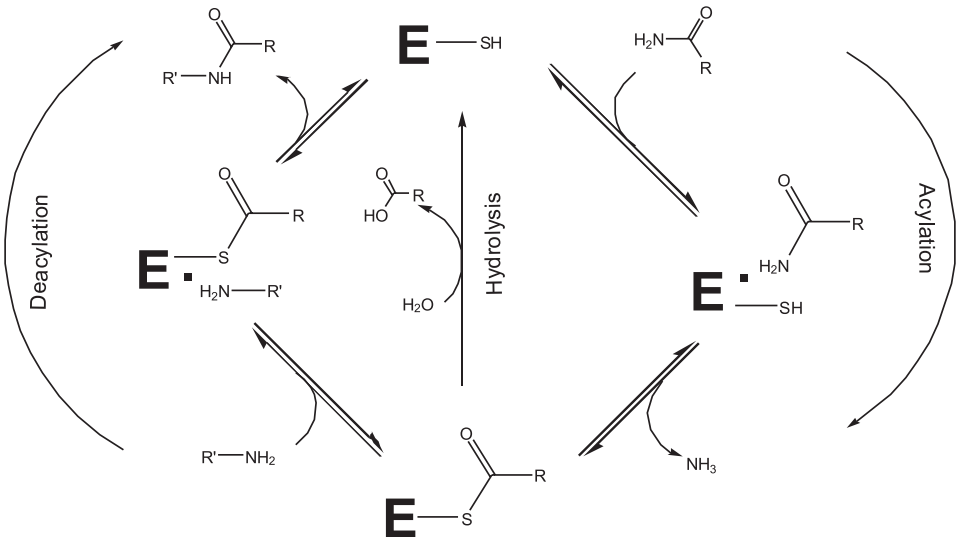

Fig. 5. Saturation kinetics of gTGase acylation by (*A*) ester **1** (squares), carbonate **2** (circles) and (*B*) thiocarbonate **3** (triangles). Each data point represents the average of 2–7 measurements. Lines through the data points were determined by non-linear regression to the hyperbolic Michaelis-Menten model (see Experimental).

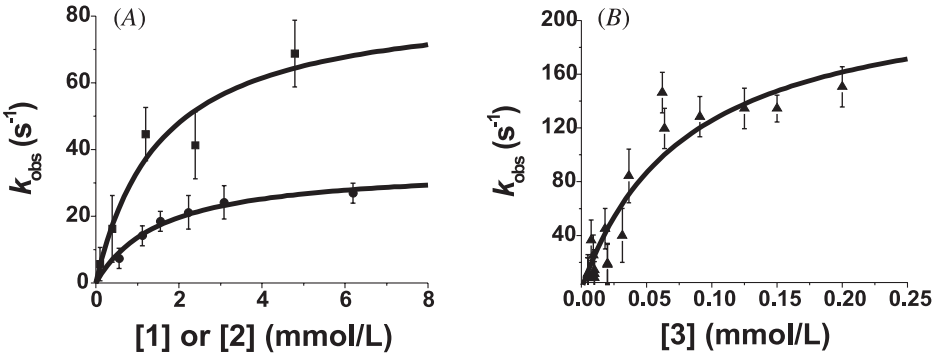

Table 2. Kinetic parameters determined for the acylation of gTGase by compounds **1**–**3** at 25 °C and pH 7.0 (0.1 mol/L MOPS).

Compound	K_M (mmol/L)	k_{acyl} (s^{-1})	k_{acyl}/K_M (mmol/L $s)^{-1}$
Ester **1**	1.5±0.8	85±15	57±40
Carbonate **2**	1.6±0.3	35±2	22±5
Thiocarbonate **3**	0.080±0.027	226±37	2800±1400

Note: Reported experimental errors are standard deviations from nonlinear regression of the data.

flected in k_{acyl}/K_M). These results go against expectations based on the reactivity of models **4**–**6** in solution. Based on the earlier discussion for thiocarbonate **6**, substrate analogue **3** was expected to be *less* reactive than ester **1** owing to its lower electrophilicity due to carbonyl-stabilizing resonance forms but *more* reactive than carbonate **2** because of the reduced resonance stabilization from carbon–sulfur orbital overlap. Clearly, other forces are at play in the enzymatic reactions of **1**–**3** that take place in a constrained, hydrophobic, and functionalized active site, compared with the model reactions of **4**–**6** that take place in free aqueous solvent.

Among these interactions are those that result in the activation of the bound substrate. Many enzymes that catalyze acyl-transfer reactions from amide groups, for example, are thought to twist the amide out of its normally planar geometry, thereby decreasing resonance stabilization and activating the carbonyl toward nucleophilic attack (43, 44). Such torsion may also be present in the Michaelis complexes formed upon binding compounds **1**–**3**. Further, one may suppose that the larger sulphur atom of thiocarbonate **3** would render it more susceptible to steric distortion, easily reducing carbon–sulphur orbital overlap and subsequently the importance of resonance stabilization. At the limit, the sulphur atom of thiocarbonate **3** would only exert an electron-withdrawing inductive effect, effectively making it a better acylating agent than the ester **1**.

Alternatively, the sulphur atom in the side chain of **3** may simply allow for better placement of the reactive carbonyl in

Fig. 6. Acylation of 2.0 μM of gTGase by 3.10 mM of carbonate **2** showing : **A**) initial burst and turnover; **B**) turnover and final loss of activity. (See Experimental.)

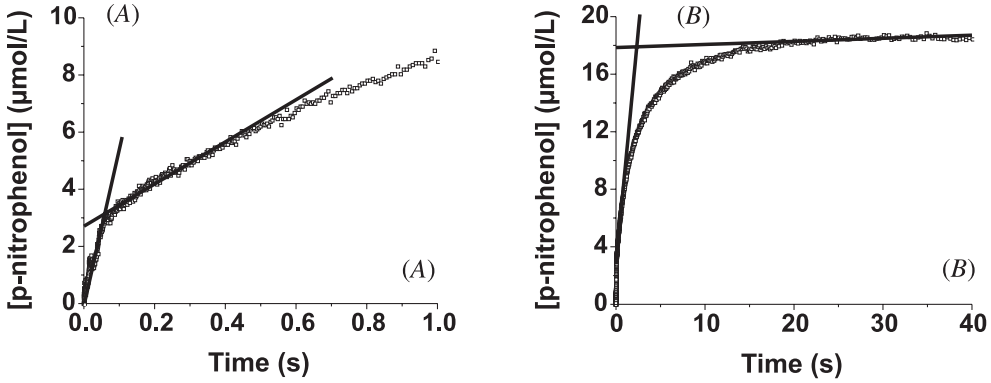

the enzyme active site. It is known that the active site of gTGase is located at the bottom of a relatively long and narrow well, allowing the enzyme to react with glutamine residues but not with asparagines (32). The introduction of a sulphur atom in the place of a methylene unit would subtly affect the bond lengths and bond angles of the side chain effectively increasing its length (45), more easily placing the acyl group within the trajectory of the active site nucleophile. Consistent with this hypothesis, we have noted that many of the irreversible glutamine-analogue gTGase inhibitors that we have synthesized in the past show greater efficiency with increasing side chain length (46, 47).

Finally, while our understanding of detailed interactions leading to substrate affinity is grossly limited by the lack of any ligand-bound crystal structure, our modelling of tissue Tgase (48) allows us to speculate why the enzyme shows increased affinity for the thiocarbonate **3**. It is known that two tryptophan residues (Trp-240 and Trp-331) and one histidine residue (His-300) form the walls of the tunnel leading the side chain to the active site. Sulphur, being a highly polarizable atom, may form favourable interactions with the faces of these aromatic residues leading to tighter binding (lower K_M), while positioning the carbonyl group to react more rapidly with the active-site thiol (higher k_{acyl}).

Inhibition kinetics

Upon closer examination of the stopped-flow traces obtained for the reaction of compounds **2** and **3** with gTGase, it was noted that over a longer time scale (up to 40 s) the slope of the "slow phase" levelled off in a nearly complete loss of activity (Fig. 6). This behaviour was not observed for ester **1**, where all of the ester substrate was consumed during the slow phase.

Knowing the final concentration of *p*-nitrophenol released prior to apparent inactivation by compounds **2** and **3** (Fig. 6*B*) allows us to estimate that the enzyme turns over ~7 times with carbonate **2** and ~4 times with thiocarbonate **3**. Apparently, all three compounds **1**–**3** initiate rapid acylation (burst phase), followed by the slower catalytic turnover of the respective acyl-enzyme (second phase). However in the case of carbonate **2** and thiocarbonate **3**, a competing event takes place that does not occur with ester **1**, leading to inhibition of the enzyme.

To characterize the inhibition, a competition experiment was carried out between ester **1** (used as the substrate) and thiocarbonate **3** (used as an inhibitor). This experiment revealed that the presence of **1** was able to temporarily protect the enzyme from inactivation by **3**, suggesting strongly that both compounds are bound in the same site. However even in the presence of ester **1**, the enzyme was still slowly inactivated by thiocarbonate **3** leading to a loss of about 50% of activity after 5 min when using 20 μmol/L of **1** (1 K_M) and 100 μmol/L of **3**. Interestingly, even after a long period (>30 min) of incubation with 100 μmol/L of thiocarbonate **3**, the addition of an aliquot of ester **1** revealed that some residual activity remained suggesting that the inactivation may be reversible. However, mass spectroscopy experiments confirmed that upon incubation with thiocarbonate **3**, the mass of gTGase increased by the expected mass of the acyl portion (see Experimental section).

Scheme 4. Two hypotheses for observed time-dependent inactivation by carbonate **2** and thiocarbonate **3**. (***A***) Two alternate binding modes or binding sites and (***B***) product inhibition.

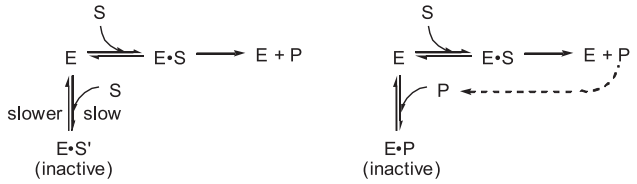

These observations led us to formulate two hypotheses regarding the inactivation mechanisms of carbonate **2** and thiocarbonate **3**. The first possibility is that both compounds **2** and **3** could have two different binding modes, one of which would lead to typical substrate-like behaviour resulting in normal turnover as for **1** (i.e., the second phase of the stopped-flow traces, Fig. 6*A*). However, an alternate binding mode for both **2** and **3** having a slow k_{on} and an even slower k_{off} would slowly lead to a tightly bound inactive form of the enzyme (see Scheme 4*A*). This binding mode could be related to the presence of a heteroatom on the side chain of **2** and **3** in the place of the methylene group of compound **1**. Examination of our tissue TGase model (48) shows that at least four gTGase residues (Trp-240, His-304, Tyr-518, and Asn-519) present a polarized hydrogen atom within <5 Å of the side chain heteroatom. The formation of a strong dipole–dipole interaction with the sulphur atom of **3**, or even a hydrogen bond with the oxygen atom of **2**, may provide the driving force for adopting an alternative tight binding mode within the active site that leads to inhibition.

Scheme 5. Difference in final product obtained after TGase-mediated hydrolysis of compounds **1**–**3** followed by subsequent decarboxylation for compounds **2** and **3**.

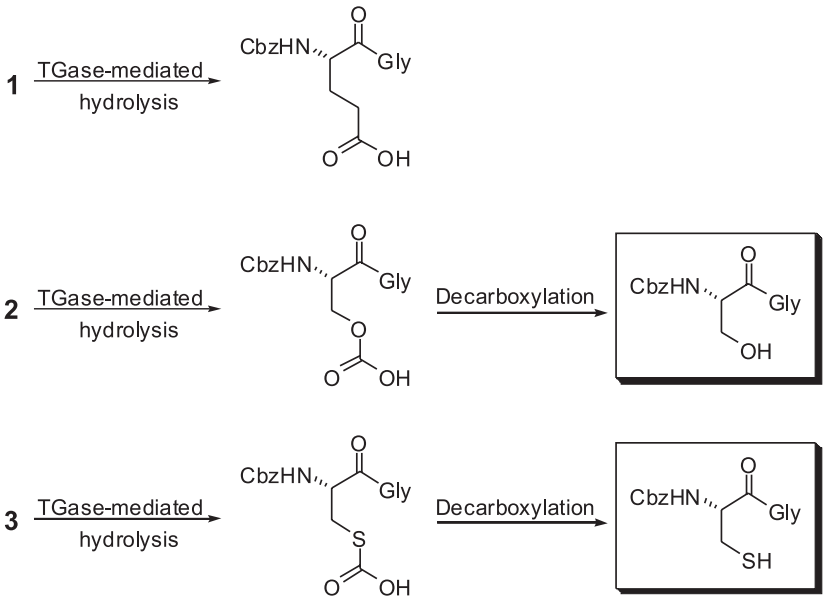

Alternatively, this different binding mode could very well be related to a different binding site, such as for example the GTP binding site, that is known to modulate the enzyme's activity through allosteric effects (12). Recently, Case and Stein (49) reported TGase inhibitors that bind either directly in this GTP binding site or in a site that regulates GTP binding. Their results also demonstrate the possibility of inhibition through the differential interaction of a given inhibitor with different conformational states of the enzyme. This further supports our hypothesis that our inhibitors may be bound by TGase at more than one site. Furthermore, putative binding at a different site could lead to acyl transfer to an adjacent nucleophile, which may explain the minor peak observed by mass spectrometry that corresponds to a doubly acylated enzyme (see Experimental section).

The second possibility is that the released product of the hydrolysis step could act as an inhibitor. Inhibition by this product would be time-dependent as its concentration increases during the catalytic turnover of its parent compound (see Scheme 4*B*). In potential support of this hypothesis, the reaction products formed after catalytic hydrolysis of **2** and **3** may undergo further spontaneous decarboxylation leading to the final products Cbz-Ser-Gly and Cbz-Cys-Gly, respectively. For example, a rate constant of 0.4 s^{-1} was recently measured under physiologically relevant reaction conditions for the decarboxylation of monoalkyl carbonate salt (50); presumably, the decarboxylation of a monoalkyl thiocarbonate would be even faster. These decarboxylation products would differ substantially from the reaction product of **1** (Scheme 5). This may explain why ester **1** showed no time-dependent inhibitory effect whatsoever.

To test this hypothesis, simple inactivation experiments were carried out in the presence of Cbz-Ser-Gly, the ultimate decarboxylated product deriving from the hydrolysis of compound **2**. No inhibition was observed, even in the presence of up to 10 mmol/L of Cbz-Ser-Gly. While this result does not strictly rule out the possibility that the hydrolysed substrate may act as an inhibitor prior to expected decarboxylation, it leads us to favour the differential binding mode hypothesis (Scheme 4*A*) as an explanation of the observed inhibition.

Conclusions

A series of gTGase substrate analogues was prepared in which the electrophilicity of the reactive carbonyl was varied by the presence of adjacent heteroatoms. Kinetic studies with model compounds provided a nonenzymatic reference for the expected rate dependence. However, the simple substitution of a side chain methylene unit by oxygen or sulphur had a surprising, counter-intuitive effect on both substrate affinity and acylation reactivity. This kinetic characterization served to illustrate the challenges associated with studying free-energy relationships in enzymatic reactions. It also provided unexpected insight into structural elements important for conferring affinity for tissue TGase as well as revealing an interesting class of irreversible inhibitors. Further work is underway to exploit these compounds as mechanistic probes and to explore their in vivo utility as inhibitors.

Materials and methods

Synthesis

General

All commercial reagents were used without further purification. Dichloromethane and tetrahydrofuran (THF) were dried using a GlassContour system (Irvine, California) column. Dry acetonitrile was bought from EM Science and used without distillation. *p*-Nitrophenyl butanoate (**4**) was purchased from Sigma-Aldrich and used without further purification. Melting points were uncorrected. Water was purified using a Millipore BioCell system.

Ethyl* p-*nitrophenyl carbonate (5)

To a suspension of sodium *p*-nitrophenolate (20 mmol) in 20 mL of anhydrous acetonitrile, a solution of ethyl chloroformate (29 mmol) in 10 mL of acetonitrile was added dropwise at 0 °C under nitrogen atmosphere. The mixture was stirred for 30 min at 0 °C and then for 3 h at room temperature (RT). Solvent was then evaporated under reduced pressure and the solid obtained was washed with dichloromethane to give 3.2 g (77%) of product as a white powder. R_f 0.74 (100% EtOAc), mp 67 to 68 °C. IR (KBr) ν: 3119, 2918, 1756, 1617, 1597, 1518, 1351, 1304, 1281. ^{1}H NMR (DMSO-d_6, 400 MHz, ppm) δ: 1.30 (3H, t, J = 7.1 Hz), 4.29 (2H, q, J = 7.1 Hz), 7.55 (2H, d, J = 9.2 Hz), 8.31 (2H, d, J = 9.2 Hz). ^{13}C NMR (DMSO-d_6, 100 MHz, ppm) δ: 14.77, 66.11, 123.50, 126.25, 145.97, 152.86, 156.17. HRMS calcd. for $C_9H_9NO_5$: 211.048 073; found: 211.048 034. Anal. calcd. for $C_9H_9NO_5$: C 51.19, H 4.30, N 6.63; found: C 51.21, H 4.50, N 6.37.

Ethyl* p-*nitrophenyl thiocarbonate (6)

To a suspension of *p*-nitrophenol (9 mmol) and pyridine (9 mmol) in 15 mL of anhydrous dichloromethane, a solution of ethyl thiochloroformate (9 mmol) in 4 mL of dichloromethane was added dropwise at 0 °C under nitrogen atmosphere. The mixture was stirred for 15 min at 0 °C and then left overnight at RT. The mixture was then extracted with 30 mL of distilled water and the organic layer was washed with 30 mL of NaOH (0.5 mol/L), 30 mL of satd. NaCl, and again with 30 mL of distilled water before being dried over $MgSO_4$ and passed through a silica gel plug using 100% $CHCl_3$ as eluant. Evaporation under reduced pressure provided 1.87 g (93.5%) of product as a white powder. R_f 0.58 (100% $CHCl_3$), mp 60 to 61 °C. IR (KBr) ν: 3084, 2973, 2936, 1708, 1621, 1590, 1532, 1490, 1347, 1098. ^{1}H NMR (DMSO-d_6, 300 MHz, ppm) δ: 1.30 (3H, t, J = 7.3 Hz), 2.97 (2H, q, J = 7.3 Hz), 7.53 (2H, d, J = 9.2 Hz), 8.30 (2H, d, J = 9.2 Hz). ^{13}C NMR (DMSO-d_6, 100 MHz, ppm) δ: 15.54, 26.32, 123.72, 126.33, 146.14, 155.98, 170.01. HRMS calcd. for $C_9H_9NO_4S$: 227.025 230; found: 227.024 816. Anal. calcd. for $C_9H_9NO_4S$: C 47.57, H 3.99, N 6.16, S 14.11; found: C 47.45, H 3.86, N 6.09, S 13.64.

N-*Benzyloxycarbonyl-*L*-serine (7)*

Sodium bicarbonate (6.3 mmol) was dissolved in 6 mL of distilled water and L-serine (0.95 mmol) was added to the solution. Once the solution was completely dissolved, benzyl chloroformate (0.63 mmol) was added dropwise at 0 °C and the mixture was stirred for 2 h at 0 °C and then overnight at RT. The aqueous phase was washed with Et_2O (4 × 5 mL) and then acidified to pH 1 with concd. HCl and extracted with EtOAc (4 × 10 mL). The combined organic layers were then washed with water, dried over $MgSO_4$, and concentrated to provide 88 mg (58%) of product as a white solid. R_f 0.054 (hexanes–EtOAc 70:30), mp 116 to 117 °C (lit. value (51) 117–119 °C). $[\alpha]_D^{20}$ +5.52° (c 1.81, HOAc) (lit. value (51) 5.8 ± 0.5° (c 2.7, HOAc)). IR (KBr) ν: 3443–2555, 3319, 3029, 2940, 1748, 1690, 1535, 1478, 1248, 1060. ^{1}H NMR (CD_3OD, 300 MHz, ppm) δ: 3.84 (1H, dd, J = 4.0 and 11.3 Hz), 3.90 (1H, dd, J = 4.9 and 11.4 Hz), 4.28 (1H, t, J = 4.4 Hz), 5.12 (2H, s), 7.29–7.39 (5H, m). ^{13}C NMR (CD_3OD, 75 MHz, ppm) δ: 56.71, 62.08, 66.71, 127.87, 128.46, 137.14, 157.60, 172.75. HRMS calc. for $C_{11}H_{13}NO_5$: 240.087 20; found: 240.088 53. Anal. calc. for $C_{11}H_{13}NO_5$: C 55.23, H 5.48, N 5.86; found: C 55.10, H 5.90, N 5.84.

N-*Benzyloxycarbonyl-*L*-serinylglycine* tert-*butyl ester (8)*

To a solution of *N*-Cbz-L-serine (**7**) (1.3 mmol) in 13 mL of anhydrous acetonitrile, diisopropylethylamine (DIEA) (5.2 mmol) was added dropwise at RT under nitrogen atmosphere, and the solution was left to stir for 5 min before glycine *tert*-butyl ester (2.6 mmol) was added. Once the solution was completely dissolved, TBTU (2.6 mmol) was added and the mixture was stirred overnight. A 50 mL aliquot of EtOAc was then added to the mixture and the organic phase was washed with saturated NaCl (2 × 15 mL), HCl (0.1 mol/L, 15 mL), 5% $NaHCO_3$ (15 mL), and again with satd. NaCl (15 mL) before being dried over $MgSO_4$, filtered, and concentrated in vacuo. The crude product was purified by flash chromatography on silica gel using 60:39:1 EtOAc–hexanes–HOAc as the eluant to provide 0.66 g (94%) of product as a white solid. R_f 0.33 (hexanes–EtOAc 30:70), mp 67–70 °C. $[\alpha]_D^{20}$ –7.71° (c 1.75, $CHCl_3$). IR (KBr) ν: 3379, 3094, 2982, 2894, 1737, 1690, 1659, 1554, 1520, 1466, 1456, 1339, 1062. ^{1}H NMR ($CDCl_3$, 300 MHz, ppm) δ: 1.47 (9H, s), 3.06 (1H, s), 3.70 (1H, dd, J = 11 and 5.4 Hz), 3.95 (2H, d, J = 5.5 Hz), 4.13 (1H, m), 4.28 (1H, m), 5.15 (2H, s), 7.30–7.42 (5H, m). ^{13}C NMR ($CDCl_3$, 75 MHz, ppm) δ: 28.37, 42.50, 63.26, 67.47, 82.79, 128.41, 128.52, 128.89, 136.57, 156.99, 169.58, 171.69. HRMS calcd. for $C_{17}H_{24}N_2O_6$: 353.171 26; found: 353.172 30. Anal. calcd. for $C_{17}H_{24}N_2O_6$: C 57.94, H 6.86, N 7.95; found: C 57.78, H 7.33, N 8.00.

N-*Benzyloxycarbonyl*-O-(p-*nitrophenoxycarbonyl*)-*L*-*serinylglycine* tert-*butyl ester (9)*

To a solution of *N*-Cbz-L-SerGly *tert*-butyl ester (**8**) (1.6 mmol) dissolved in 5 mL of anhydrous acetonitrile, pyridine (7.9 mmol) was added dropwise under nitrogen. The solution was stirred for a few minutes and was then placed in an ice bath. At 0 °C, *p*-nitrophenyl chloroformate (1.6 mmol) was then added and the bath removed while the mixture was stirred for 3 h. A 20 mL volume of EtOAc was added and the organic layer was washed with HCl (3 mmol/L, 3 × 10 mL), dried over $MgSO_4$, filtered, and concentrated in vacuo. The crude product was purified by flash chromatography on silica gel using 30:70 EtOAc–hexanes as the eluant. A 0.51 g (63%) quantity of the product was obtained as a white powder that could be recrystallized from CH_2Cl_2–hexanes. R_f 0.37 (hexanes–EtOAc 60:40), mp 52–54 °C. $[\alpha]_D^{20}$ +6.87° (c 1.50, $CHCl_3$). IR (KBr) ν: 3317, 3085, 2980, 2939, 1773, 1737, 1729, 1670, 1594, 1349, 1554, 1520, 1493, 1455, 1214, 1049. ^{1}H NMR ($CDCl_3$, 300 MHz, ppm) δ: 1.47 (9H, s), 3.96 (2H, s), 4.51 (1H, dd, J = 11.1 and 4.7 Hz), 4.65 (1H, dd, J = 11.0 and 5.3 Hz), 4.72 (1H, m), 5.17 (2H, d, J = 12.0 Hz), 5.79 (1H, s), 6.83 (1H, s), 7.27–7.37 (7H, m), 8.25 (2H, d, J = 9.1 Hz). ^{13}C NMR ($CDCl_3$, 75 MHz, ppm) δ: 28.45, 42.59, 53.90, 68.07, 68.66, 83.25, 122.26, 125.76, 128.65, 128.89, 129.08, 145.94, 152.60, 155.71, 156.55, 156.67, 168.55, 168.90. HRMS calcd. for $C_{24}H_{27}N_3O_{10}$: 518.177 49; found:

518.176 30. Anal. calcd for $C_{24}H_{27}N_3O_{10}$: C 55.70, H 5.26, N 8.12; found: C 55.03, H 5.33, N 8.04.

N-*Benzyloxycarbonyl*-O-*(*p-*nitrophenoxycarbonyl)-*L-*serinylglycine (2)

To a solution of *N*-Cbz-*O*-(*p*-nitrophenoxycarbonyl)-L-serinylglycine *tert*-butyl ester (**9**) (0.4 mmol) in 2.5 mL of anhydrous dichloromethane, 500 µL (6.5 mmol) of trifluoroacetic acid (TFA) was added dropwise at 0 °C under nitrogen atmosphere. The solution was stirred at 0 °C for 1 h and then an additional portion (300 µL, 4.0 mmol) of TFA was added and the solution was stirred for an additional 3 h while the solution was allowed to warm to RT. A final portion of 150 µL of TFA (2.0 mmol) was then added and the solution was stirred at RT for 1 h before the solvent was removed in vacuo to provide 0.165 g (92%) of product as a yellow solid. R_f 0.28 (99:1 EtOAc–HOAc), mp 59–61 °C. $[\alpha]_d^{20}$ +11.0° (c 0.96, $CHCl_3$). IR (KBr) ν: 3747–2633, 3086, 2968, 1772, 1740, 1734, 1640, 1595, 1351, 1526, 1493, 1455, 1279, 1049. ^{1}H NMR ($CDCl_3$, 300 MHz, ppm) δ: 4.12 (2H, d, $J \approx 17$ Hz), 4.50 (1H, dd, J = 4.5 (3.8) and 10.7 Hz), 4.60 (1H, dd, J = 6.5 (5.8) and 10.9 Hz), 4.82 (1H, m), 5.15 (2H, d, J = 11.8 Hz), 5.84 (1H, s), 7.10 (1H, s), 7.29–7.39 (7H, m), 8.26 (2H, d, J = 9.2 Hz). ^{13}C NMR ($CDCl_3$, 75 MHz, ppm) δ: 41.81, 53.80, 68.17, 68.63, 122.19, 125.72, 128.50, 128.93, 129.05, 135.91, 145.90, 152.69, 155.53, 157.07, 169.74, 172.68. HRMS calcd. for $C_{20}H_{19}N_3O_{10}$: 462.114 87; found: 462.116 50. Anal. calcd. for $C_{20}H_{19}N_3O_{10}$: C 52.06, H 4.15, N 9.11; found: C 50.33, H 4.20, N 8.41.

N-*Benzyloxycarbonyl*-L-*cystine (10)*

To 1.44 g (5.94 mmol) of L-cystine in 175 mL of water was added 5 g (60 mmol) of $NaHCO_3$ and the mixture was cooled to 0 °C. A 1.70 mL volume (13.0 mmol) of benzyl chloroformate was added dropwise and the biphasic solution was stirred vigorously overnight. After acidification to pH 3 using 6N HCl, the aqueous phase was extracted with 3 × 150 mL EtOAc and the extract was concentrated in vacuo to give 3.38 g (99%) of a clear oil. R_f 0.05 (50:50 EtOAc–hexanes). ^{1}H NMR (CD_3OD, 300 MHz, ppm) δ: 2.98 (1H, dd, J = 9.1 and 13.9 Hz), 3.25 (1H, dd, J = 4.3 and 13.9 Hz), 4.51 (1H, dd, J = 4.3 and 9.1 Hz), 5.07 (2H, s), 7.27 (5H, m). ^{13}C NMR (CD_3OD, 75 MHz, ppm) δ: 41.18, 54.71, 67.81, 128.84, 129.03, 129.51, 139.09, 158.54, 174.02.

N-*Benzyloxycarbonyl*-L-*cystinylglycine* tert-*butyl ester (11)*

A 3.38-g (6.6 mmol) portion of *N*-benzyloxycarbonyl-L-cystine (**10**) and 5.76 mL (33 mmol) of DIEA were dissolved in 120 mL of anhydrous acetonitrile. To this solution was added 2.76 g (17 mmol) of glycine *tert*-butyl ester hydrochloride and 6.36 g (20 mmol) of TBTU. The mixture was stirred overnight. The next day, 120 mL of EtOAc was added and the organic phase was washed with 3 × 120 mL satd. NaCl, 100 mL 1N NaOH, and 100 mL H_2O. After concentration in vacuo and purification by silica gel chromatography (15 cm × 2.5 cm, 33% EtOAc–toluene), 2.91g (60%) of a white solid was obtained. R_f 0.43 (50:50 EtOAc–hexanes). ^{1}H NMR ($CDCl_3$, 300 MHz, ppm) δ: 1.42 (9H, s), 2.87 (1H, dd, J = 11 and 15 Hz), 3.10 (1H, dd, J = 15 and 4 Hz), 3.77 (1H, dd, J = 18 and 5 Hz), 4.00 (1H, dd, J = 18 and 5 Hz), 5.10 (1H, m), 5.16 (2H, s), 5.8 (1H, d, J = 9 Hz), 7.31 (5H, m), 7.95 (1H, t, J = 5 Hz). ^{13}C NMR ($CDCl_3$, 75 MHz, ppm) δ: 27.90, 41.93, 46.04, 55.10, 67.15, 81.98, 127.50, 127.97, 128.37, 136.30, 156.87, 168.27, 170.02. HRMS calcd. for $C_{34}H_{46}N_4O_{10}S_2$ + H: 735.272 81; found: 735.272 07.

N-*Benzyloxycarbonyl*-L-*cysteinylglycine* tert-*butyl ester (12)*

A 100-mg (0.136 mmol) portion of *N*-benzyloxycarbonyl-L-cystinylglycine *tert*-butyl ester (**11**) and 100 mg (2.6 mmol) of sodium borohydride were dissolved in a mixture of 2 mL of ethanol and 2 mL of $CHCl_3$. The mixture was shaken for 30 min at RT. Then, 5 mL of $CHCl_3$ was added and the organic phase was washed with HCl (10 mL, 1 mol/L) and then concentrated in vacuo. If necessary, the product can then be purified by silica gel chromatography using 30:70 EtOAc–hexanes as eluant. To avoid oxidation, the last step was carried out immediately. R_f 0.50 (50:50 EtOAc–hexanes). ^{1}H NMR ($CDCl_3$, 300 MHz, ppm) δ: 1.17 (3H, s), 1.42 (1H, dd, J = 8.4 and 11.4 Hz), 2.58 (1H, ddd, J = 15.2, 11.4, and 6.6 Hz), 2.97 (1H, ddd, J = 15.2, 8.4, and 5.1 Hz), 3.87 (2H, d, J = 6.2 Hz), 4.50 (1H, m), 5.19 (2H, s), 6.04 (1H, d, J = 9.2 Hz), 7.11 (1H, t, J = 6.2 Hz), 7.61 (5H, m). ^{13}C NMR ($CDCl_3$, 75 MHz, ppm) δ: 27.91, 41.92, 46.14, 55.12, 67.02, 81.95, 127.80, 127.92, 128.74, 136.25, 156.92, 168.32, 170.06.

N-Benzyloxycarbonyl*-S-*(*p-*nitrophenyloxycarbonyl)-*L-*cysteinylglycine* tert-*butyl ester (13)

First, 110 mg (0.3 mmol) of *N*-benzyloxycarbonyl-L-cysteinylglycine *tert*-butyl ester (**12**) and 104 µL of DIEA were dissolved in 0.5 mL of $CHCl_3$ at 0 °C. Then, 60 mg (0.3 mmol) of *p*-nitrophenyl chloroformate dissolved in 0.5 mL of $CHCl_3$ was added at 0 °C and the mixture was shaken for 15 min. The mixture was then purified by silica gel chromatography using 1:2 EtOAc–hexanes. The product was obtained as 68 mg (68%) of a yellow solid. R_f 0.50 (1:1 EtOAc–hexanes). ^{1}H NMR ($CHCl_3$, 300 MHz, ppm) δ: 1.18 (3H, s), 3.19 (1H, dd, J = 6.4 and 13.5 Hz), 3.37 (1H, dd, J = 4.1 and 13.5 Hz), 3.88 (2H, d, J = 4.0 Hz), 4.70 (1H, dd, J = 4.1 and 6.4 Hz), 5.23 (1H, d, J = 13.2 Hz), 5.27 (1H, d, J = 13.2 Hz), 5.80 (1H, d), 6.95 (1H, t), 7.56 (2H, d, J = 10.5 Hz), 7.62 (5H, m), 8.58 (2H, d, J = 10.5). ^{13}C NMR ($CDCl_3$, 75 MHz, ppm) δ: 28.2, 28.5, 43.3, 53.2, 65.2, 122.2, 124.8, 127.2, 127.3, 127.8, 136.6, 145.1, 155.1, 155.4, 167.3, 168.0, 169.9.

N-*Benzyloxycarbonyl*-S-*(*p-*nitrophenyloxycarbonyl)-*L-*cysteinylglycine (3)

To 34 mg (64 µmol) of *N*-benzyloxycarbonyl-*S*-(*p*-nitrophenoxycarbonyl)-L-cysteinylglycine *tert*-butyl ester (**13**) dissolved in 2 mL of chloroform was added 500 µL (6.5 mmol) of TFA at 0 °C. The solution was stirred for 1 h and then evaporated in vacuo. The product thus obtained was used without further purification. R_f 0.12 (50:50 EtOAc–hexanes). ^{1}H NMR ($CHCl_3$, 400 MHz, ppm) δ: 3.10 (1H, dd, J = 6.3 and 13.6 Hz), 3.26 (1H, dd, J = 4.1 and 13.6 Hz), 4.05 (2H, d, J = 3.8 Hz), 4.82 (1H, dd, J = 4.1 and 6.3 Hz), 5.23 (1H, d, J = 13.1 Hz), 5.27 (1H, d, J = 13.1 Hz), 6.30 (1H, d, J = 8.1 Hz), 7.56 (2H, d, J = 10.5 Hz), 7.62 (5H, m), 7.87

(1H, t), 8.58 (2H, d, J = 10.5). ^{13}C NMR ($CDCl_3$, 75 MHz, ppm) δ: 28.0, 43.3, 53.2, 65.1, 122.2, 124.9, 127.2, 127.3, 127.8, 136.4, 145.0, 155.2, 155.4, 167.3, 168.0, 171.7. HRMS calcd, for $C_{20}H_{19}N_3O_9S$ + H: 478.091 48; found: 478.092 51.

TGase expression and purification

TGase was obtained according to a previously published procedure developed in the group (8). Enzyme activity was determined using the hydroxamate assay (52).

Pre-equilibrium kinetics

A buffer solution containing MOPS (110 mmol/L), $CaCl_2$ (3.3 mmol/L), and EDTA (55 mmol/L) was adjusted to pH 7.0. The enzymatic solution was prepared by dissolving approximately 1.5 mg of lyophilized gTGase in 6 mL of buffer solution. Protein concentration was measured using the D_C Protein Assay from BioRad (Mississauga, Ontario) and verified to be approximately 0.25 mg/mL in all cases. Stock substrate solutions were prepared by dissolving a known quantity of compound **1**, **2**, or **3** into dry, degassed acetonitrile. All pre-equilibrium kinetic data were collected using a SX.18MV stopped-flow reaction analyser from Applied Photophysics (London, UK). Measurements for the single mixing stopped-flow method were taken at an absorption wavelength of 410 nm. The injection syringes were of 2.5 mL volume for the enzyme solutions and of 0.25 mL volume for the substrate solution, ensuring a 1:10 mixing ratio resulting in final concentrations of 100 mnol for MOPS, 3 mmol/L for $CaCl_2$, 50 μmol/L for EDTA, and 10% acetonitrile. The optical path within the cell was 10 mm. The temperature was kept at 25 °C using an Isotemp 1016P bath from Fisher Scientific. All kinetic runs were corrected for background absorption from the buffer and substrate solutions. Pre-steady state and initial steady state rates were measured by linear regression over time ranges up to and from the obvious inflection point to give a linear correlation of at least R^2 = 0.99. Finally, all runs were corrected for nonenzymatic background hydrolysis by subtracting from each the final slope of the value obtained in the control experiments in which no TGase was used. Ensuing Michaelis–Menten plots were fit to the standard hyperbolic equation. All linear and nonlinear regression was performed using Microcal™ Origin® 6.0 software from Microcal Software, Inc.

Nonenzymatic hydrolysis kinetics

All measurements were made using a UV–vis Cary Varian 100 Bio spectrophotometer and disposable polystyrene cells. Final conditions in each cuvette were MOPS (0.1 mol/L, pH 7), μ = 0.2 mol/L (KCl) and a variable quantity of either ethanethiol or cysteamine, ranging from 10 to 60 mmol/L. Reactions were initiated by adding 50 μL of a DMF solution of acyl-transfer reactant to 950 μL of buffered thiol solution, resulting in an initial reactant concn. of 0.13 mmol/L. The release of *p*-nitrophenol was followed at 410 nm and absorbance data were fitted to a monoexponential equation ($Abs_t = Abs_\infty(1 - \exp[-k_{obs}t])$). The extinction coefficient for *p*-nitrophenolate at 25 °C and pH 7 was determined experimentally to be 8040 $(mol/L)^{-1}$ cm^{-1} (22). Correction for background hydrolysis was obtained by simultaneously running control experiments in absence of nucleophile in a second cell, while using the dual beam function of the instrument.

Mass spectroscopy

A solution of TGase (5 μmol/L), **3** (25 mmol/L), $CaCl_2$ (3 mmol/L), and EDTA (50 μmol/L) in Tris buffer (0.1 mol/L, pH = 7.0) was incubated for 15 min at 25 °C. Aliquots were withdrawn and injected on an Agilent HPLC-MS (1100 series, MSD TOF) equipped with a Poroshell 300SP-C8 column and running a 0.35 mL/min flow rate acetonitrile gradient (0 min, 20%; 6 min, 100%; 7 min, 100%; 7.2 min, 20%; 12 min, 20%). Protein was detected after 4.74 min and deconvolution showed a m/z ratio of 78 890 Da for the inhibitor-free sample of His-tagged enzyme. For the sample obtained after incubation in the presence of inhibitor, m/z ratios of 79 229 Da (major) and 79 568 Da (minor) were found, consistent with the expected mass increase due to addition of the acyl moiety of **3**.

Acknowledgments

This work was supported by the Natural Sciences and Engineering Research Council (NSERC) of Canada. CG and DL thank NSERC for postgraduate scholarships, and CG and JL thank the Fonds Québecois de Recherche sur la Nature et les Technologies (FQRNT) for postgraduate scholarships.

References

1. D. Aeschlimann and M. Paulsson. Thromb. Haemostasis, **71**, 402 (1994).
2. C.S. Greenberg, P.J. Birckbichler, and R.H. Rice. FASEB J. **5**, 3071 (1991).
3. N. Takahashi, Y. Takahashi, and F.W. Putnam. Proc. Natl. Acad. Sci. USA. **83**, 8019 (1986).
4. M.A. Philips, B.E. Stewart, Q. Qin, R. Chakravarty, E.E. Floyd, A.M. Jetten, and R.H. Rice. Proc. Natl. Acad. Sci. USA. **87**, 9333 (1990).
5. K.C. Ho, V.E. Quarmby, F.S. French, and E.M. Wilson. J. Biol. Chem. **267**, 12660 (1992).
6. S.-Y. Kim, I.-G. Kim, S.-I. Chung, and P.M. Steinert. J. Biol. Chem. **269**, 27979 (1994).
7. W. Dietrich, T. Ehnis, M. Bauer, P. Donner, U. Volta, E.O. Riecken, and D. Schupann. Nature Med. **3**, 797 (1997).
8. S.M.F.G. Gillet, R.A. Chica, J.W. Keillor, and J.N. Pelletier. Protein Expression Purif. **33**, 256 (2004).
9. K. Ikura, T. Nasu, H. Yokota, Y. Tsuchiya, R. Sasaki, and H. Chiba. Biochemistry, **27**, 2898 (1988).
10. A.N. Glazer and E.L. Smith. The Enzymes. Academic Press, New York. 1971.
11. H.-C. Kim, Z. Nemes, W.W. Idler, C.C. Hyde, P.M. Steinert, and B.J. Ahvazi. J. Struct. Biol. **135**, 73 (2001).
12. S. Liu, R.A. Cerione, and J. Clardy. Proc. Natl. Acad. Sc. USA. **99**, 2743 (2002).
13. K. Noguchi, K. Ishikawa, K.-I. Yokoyama, T. Ohtsuka, N. Nio, and E.-I. Suzuki. J. Biol. Chem. **276**, 12055 (2001).
14. J.E. Folk. J. Biol. Chem. **244**, 3707 (1969).
15. P.H. Jensen, E.S. Sorensen, T.E. Petersen, J. Gliemann, and L.K. Rasmussen. Biochem. J. **310**, 91 (1995).
16. W. Borth, V. Chang, P. Bishop, and P. Harpel. J. Biol. Chem. **268**, 18149 (1991).

17. O. Molberg, S.N. McAdam, R. Korner, H. Quarsten, C. Kristiansen, L. Madsen, L. Fugger, H. Scott, O. Noren, P. Roepstorff, K.E.A. Lundin, H. Sjostrom, and L.M. Sollid. Nature Med. **4**, 713 (1998)
18. S. Reif and A. Lerner. Autoimmun. Rev. **3**, 40 (2004).
19. P.J.T.A. Groenen, J.J. Grootjans, N.H. Lubsen, H. Bloemendal, and W.W. Jong. J. Biol. Chem. **269**, 831 (1994).
20. S. Igarashi, R. Koide, T. Shimohata, M. Yamada, Y. Hayashi, H. Takano, H. Date, M. Oyake, T. Sato, A. Sato, S. Egawa, T. Ikeuchi, H. Tanaka, I. Hozumi, I. Inuzuka, H. Takahashi, and S. Tsuji. Nat. Genet. **18**, 111 (1998).
21. A.J.L. Cooper, K.R. Sheu, J.R. Burke, O. Onodera, W.J. Strittmatter, A.D. Roses, and J.P. Blass. J. Neurochem. **69**, 431 (1997).
22. A. Leblanc, C. Gravel, J. Labelle, and J.W. Keillor. Biochemistry, **40**, 8335 (2001).
23. H. Sato, N. Yamada, N. Shimba, and Y. Takahara. Anal. Biochem. **281**, 68 (2000).
24. L. Shan, O. Molberg, I. Parrot, F. Hausch, F. Filiz, G.M. Gray, L.M. Sollid, and C. Khosla. Science (Washington, D.C.), **297**, 2275 (2002).
25. D.J. Verrinder, M.J. Hourigan, and J.M. Prokipcak. Can. J. Chem. **56**, 2582 (1978).
26. E.A. Castro, F. Ibanez, S. Lagos, M. Schick, and J.G. Santos. J. Org. Chem. **57**, 2691 (1992).
27. E.A. Castro, P. Pavez, and J.G. Santos. J. Org. Chem. **66**, 3129 (2001).
28. E.A. Castro, P. Pavez, and J.G. Santos. J. Org. Chem. **67**, 4494 (2002).
29. E.A. Castro, P. Pavez, and J.G. Santos. J. Org. Chem. **68**, 9034 (2003).
30. S.L. Shames and L.D. Byers. J. Am. Chem. Soc. **103**, 6170 (1981).
31. S.I. Chung, R.I. Shrager, and J.E. Folk. J. Biol. Chem. **245**, 6424 (1970).
32. T. Ohtsuka, M. Ota, N. Nio, and M. Motoki. Biosci. Biotechnol. Biochem. **64**, 2608 (2002).
33. J.E. Folk and S.I. Chung. Adv. Enzymol. Relat. Areas Mol. Biol. **38**, 109 (1973).
34. P. Adams and F.A. Baron. Chem. Rev. **65**, 567 (1965).
35. D.J. Woodcock. Chem. Comm. (London), 267 (1968).
36. A.F. Hegarty and L.N. Frost. Chem. Comm. 500 (1972).
37. A.F. Hegarty and L.N. Frost. J. Chem. Soc. Perkin Trans. 2, 1719 (1973).
38. M.I. El Seoud and O.A. El Seoud. J. Org. Chem. **46**, 2286 (1981).
39. S.M. Rahmathullah, J.E. Hall, B.C. Bender, D.R. McCurdy, R.R. Tidwell, and D.W. Boykin. J. Med. Chem. **42**, 3994 (1999).
40. W.P. Jencks and K. Salvesen. J. Am. Chem. Soc. **93**, 4433 (1971).
41. R.E. Benesch and R.J. J. Benesch. J. Am. Chem. Soc. **77**, 5877 (1955).
42. J.W. Keillor and R.S. Brown. J. Am. Chem. Soc. **114**, 7983 (1992).
43. K.I. Skorey and R.S. Brown. J. Am. Chem. Soc. **107**, 4070 (1985).
44. M. Morin, C. Rivard, and J.W. Keillor. Org. Biomol. Chem., **4**, 3790 (2006).
45. A. Planas and J.F. Kirsch. Biochemistry, **30**, 8268 (1991).
46. C. Marrano, P. de Macédo, P. Gagnon, D. Lapierre, and J.W. Keillor. Bioorg. Med. Chem. **9**, 3231 (2001).
47. C. Marrano, P. de Macédo, and J.W. Keillor. Bioorg. Med. Chem. **9**, 1923 (2001).
48. R.A. Chica, P. Gagnon, J.W. Keillor, and J.N. Pelletier. Protein Sci. **13**, 979 (2004).
49. A. Case and R.L. Stein. Biochemistry, **46**, 1106 (2007).
50. G. Papageorgiou, A. Barth, and J.E.T. Corrie. Photochem. Photobiol. Sci. **4**, 216 (2005).
51. Handbook of fine chemicals and laboratory equipment. Sigma-Aldrich Company, 2000–2001.
52. J.E. Folk, and S.I. Chung. Methods Enzymol. **113**, 358 (1985).